Terahertz/optical sum and difference frequency generation in liquids

Thomas Feil[1,2,a)] and S. J. Allen[2]
[1]*Institut für Festkörperphysik, ETH Zürich, 8093 Zürich, Switzerland*
[2]*Institute for Terahertz Science and Technology, UCSB, Santa Barbara, California 93106, USA*

(Received 18 June 2010; accepted 18 January 2011; published online 9 February 2011)

A high-sensitivity setup for the observation of $\chi^{(2)}$-based, terahertz/optical, sum and difference frequency generation in liquids is presented. It relies on launching wavefront modulated terahertz radiation into a liquid traversed by an optical beam. Phase matching and polarization selection rules can be tuned to support three wave mixing via either chiral allowed electric dipole processes or higher order quadrupole/magnetic dipole processes. Under nonresonant excitation, hyperpolarizabilities from quadrupole/magnetic dipole processes are measured. Since this approach does not require terahertz transmission through macroscopic thicknesses of water, it has the potential to open a new window on the terahertz dynamics of water solvated molecules. © *2011 American Institute of Physics*. [doi:10.1063/1.3552964]

Chiral sum and difference frequency generation (SDFG) has been shown to be a competitive tool for the vibrational spectroscopy of liquids and solutions[1,2] in the infrared frequency band. To explore the lowest frequency macromolecular modes of biomolecules, which occur at terahertz frequencies, in life's natural environment—water, we have developed a high-sensitivity approach for detecting nonlinear mixing of terahertz and optical radiation in liquids. This approach is motivated by the difficulty encountered doing conventional terahertz absorption spectroscopy caused by the overwhelming absorption of the water solvent.[3–7] Furthermore, we wish to exploit the fact that nonlinear, sum and difference frequency generation, a $\chi^{(2)}$-process, is largely suppressed in liquids but may be activated by the intrinsic chiral symmetry of biomolecules.[8] The approach described in the following letter has the potential for circumventing the strong terahertz absorption of the solvent, potentially select for chiral biomolecules, and be doubly resonant with electronic excitations and macromolecular vibrations.

A configuration that optimizes SDFG in the face of strong terahertz absorption by water is shown in Fig. 1. A metal grating (gold) of period $d=2\pi/k_G$ is fabricated on top of a terahertz transparent substrate (here semi-insulating GaAs). This substrate is surrounded by a cuvette, which contains the liquid. Terahertz radiation (electric field vector E_{THz}) from the UCSB free electron laser (FEL) is focused onto the plane of the gold grating with a diameter equal to the width of the cuvette opening. At the same time, visible radiation, provided by a 532 nm multimode, flashlamp pumped yttrium-aluminum-garnet (YAG) laser (electric field vector E_0), is guided through the liquid just above the grating surface. With reference to the schematic drawing in Fig. 1(b), the optical beam has an elliptical cross section z_0 $=50$ μm high$\times 1$ mm wide. Alignment is critical and is achieved by blocking the optical beam by a piece of etched GaAs. The surface of the 2 mm thick GaAs in contact with the grating has a 50 μm deep trough 2 mm wide, forming a 50 μm high "tunnel" at the grating surface. Alignment is tested by assuring that 90% of the aforementioned elliptical beam passes through the tunnel, especially as the grating is rotated.

The two lasers overlap in the liquid above the metal grating. Efficient nonlinear conversion requires phase matching[9] according to $\vec{k}_{\pm}-\vec{k}_0-\vec{k}_G=0$, where $\vec{k}_0$ and $\vec{k}_{\pm}$ are the wavevectors of the incoming 532 nm light and the sum or difference frequency radiation (electric field vector $E_{\pm}$), respectively. For the current planar process, this results in the following equations [cf. Fig. 1(c)]:

$$k_G \cos(\theta_G-\theta)+n_s k_0 = n_s k_{\pm}\cos(\delta\theta), \tag{1}$$

$$k_G \sin(\theta_G-\theta) = n_s k_{\pm}\sin(\delta\theta). \tag{2}$$

By allowing the grating to rotate in the x-y-plane, θ_G can be adjusted to meet these conditions for a (well) chosen grating period d. As the cuvette rotates with the grating, the incident radiation is refracted through an angle θ and the effective grating angle is $\theta_G-\theta=\theta_G-\arcsin[\sin(\theta_G)/n_s]$, where n_s is the optical refractive index of the liquid. The visible laser excitation has a very narrow spatial width of 50 μm perpendicular to the grating (1 mm in the grating plane). This essentially confines the nonlinear process to the x-y-plane. The sideband radiation, very nearly collinear with the exciting radiation ($\delta\theta$ is very small), is collected and spectrally resolved in a double monochromator. As shown in Fig. 1(b), the sideband radiation is polarized perpendicular to that of the incoming beam. Therefore, a set of crossed polarizers [Pol 1 and Pol 2 in Fig. 1(b)] around the mixing chamber

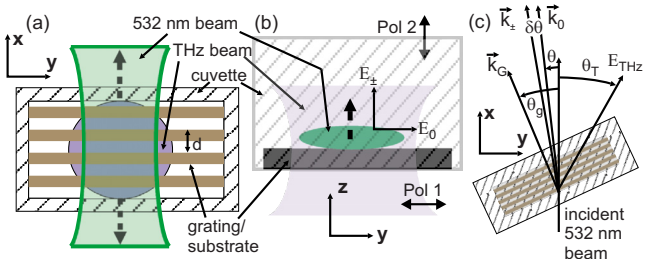

FIG. 1. (Color online) Measurement setup. (a) Top view—the terahertz radiation is incident from below the grating, normal to the page. (b) Side view—E_0 and $E_{\pm}$: electric fields of 532 nm excitation and SDFG signal; Pol 1, Pol 2: polarizer before and behind the interaction volume. (c) Wavevectors for phase matching and terahertz polarization in the plane of the grating.

a)Electronic mail: tfeil@phys.ethz.ch.

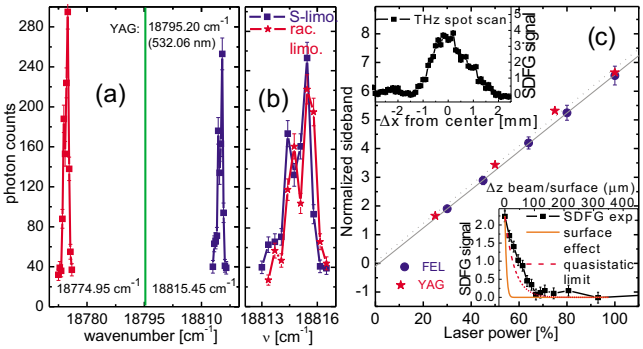

FIG. 2. (Color online) (a) SDFG in S-limonene at 0.615 THz with a $d=354$ μm grating at $\theta_G=27°$. (b) Sum frequency generation (SFG) for S-limonene and a racemic mixture of limonene. (c) Power dependence of the limonene SFG signal, showing that it is a linear function of both terahertz and optical power. (Inset top) Sideband signal dependence for terahertz spot scan along the x-axis. (Inset bottom) Sideband signal dependence for increased separation between grating surface and 532 nm beam.

allows one to suppress the exciting 532 nm light by four to five orders of magnitude before it enters the spectrometer. This, combined with very narrow spectrometer slits, delivers a signal to background ratio for the strongest observed sidebands of about 100. While the remaining background currently limits the reliably detectable signal strength, we are nonetheless able to observe nonresonant, $\chi^{(2)}$-based, terahertz/visible SDFG in liquids. The signal is detected with a photomultiplier tube by photon counting or averaged, time resolved, current transients. Under the conditions described in Eqs. (1) and (2), the entire interaction volume defined by the overlap of the terahertz and optical beams is phase matched to optimize the power radiated at the sum or difference frequency.

In the following, the SDFG process is characterized through the geometry and phase matching dependencies in the setup using enantiomeric and racemic limonene as a medium. In *completely identical geometries*, all measured sidebands disappear without the liquid. The FEL is tuned to frequencies around 0.65 THz and delivers output powers of about 1–2 kW in a narrow, ~1–3 μs, pulse at a repetition rate of the order of ~1 Hz. Figure 2(a) shows scans across the sum and difference frequency sidebands around the 532 nm (18 795.2 cm^{-1}) YAG line generated in S-limonene by 0.61 THz (20.3 cm^{-1}). The rotation angle was 27°. At each point, 500 mixing events are averaged. Due to the narrow monochromator slit widths (50 μm), individual features of the multimode line of the YAG laser are partially resolved. In the following, signals are extracted as the integral of the total sideband line.

Sum frequency sidebands for both S-limonene and a racemic limonene mixture are compared in Fig. 2(b). Within the accuracy of the experiment, there is no appreciable difference. Since the racemic mixture is nonchiral, the observed sidebands can originate from a $\chi^{(2)}$ origin beyond the dipole approximation or be due to higher even order polarizations. The linear power dependences of the limonene sideband, shown in Fig. 2(c), excludes the latter. The nonlinear polarization is thus caused by magnetic dipolar or quadrupolar processes.

It is important to distinguish volume from surface generated nonlinear polarization. Molecules in a surface layer may not enjoy the full rotational invariance of the liquid and may turn on a $\chi^{(2)}$ process. In addition, the abrupt termination of the three radiation fields at the surface can activate quadrupole or magnetic dipole processes at the surface. Indeed, much published work has focused on distinguishing three wave mixing due to surface molecular layers and bulk quadrupole and magnetic dipole effects that are caused by the surface boundary conditions of the three waves.[10]

We performed two control measurements to discriminate against mixing at interfaces. We do so by scanning the interaction volume defined by the terahertz and optical beam overlap. Before doing so, we independently established the size of the terahertz and optical beams. First, the terahertz spot was scanned along the x-axis in the volume above the grating [see arrow Fig. 1(a)]. The strong signal at the grating center in the top inset of Fig. 2(c) precludes mixing on the vertical cuvette sidewalls, consistent with a volume effect. To explore the possibility that the SDFG arises from the surface of the grating, we measured the signal as a function of the height of the optical beam above the grating [dashed line in Fig. 1(b)]. The results are displayed and compared to two models in the lower inset in Fig. 2(c). One model assumes that the mixing occurs in molecules adsorbed on the surface. Signals from these molecules will decay at a rate controlled by the vertical Gaussian width of the optical beam. The predicted decay is very much faster than that observed (a ratio of 2.5×10^{-7} at $\Delta z=50$ μm). The other model assumes that the drop off of sideband intensity is due to the decay of the grating induced spatial modulation of the terahertz field in the quasistatic limit $\lambda_{THz}\gg d$, SDFG $\sim\exp[-4\pi\cos(\theta_G)(z_0/2+\Delta z)/d]$. It predicts a just slightly faster attenuation than observed. However, we are strictly not in the quasistatic limit ($\lambda_{THz}\sim d$) and more rigorous models that capture shadowing would lead to a slower decay of the spatially modulated intensity. The measured decay when compared with these two models strongly supports mixing in the bulk, a volume effect.

A nonlinear quadrupolar process[11] in an isotropic medium produces a *local* polarization, $d\vec{P}$, at the sum or difference frequency that is proportional to the following vector product[12] (the radiation from a second term $\propto\vec{E}_0$ is suppressed by the cross polarizers):

$$d\vec{P}(\omega_{THz}\pm\omega_0)\propto[(\vec{k}_G+\vec{k}_0)\cdot\vec{E}_0]\vec{E}^G_{THz}. \tag{3}$$

Here, $\vec{E}^G_{THz}$ is the terahertz electric field above and in the near field of the grating [see inset in Fig. 3(a)]. It is spatially modulated at the grating period and there are spatially modulated components both perpendicular to the grating surface as well as along the grating wavevector; there are none along the grating lines. As the relative orientation of the incident terahertz field, $\vec{E}_{THz}$, and grating wavevector, $\vec{i}_G$, are altered, the magnitude of the modulated terahertz field will vary as $|\vec{E}^G_{THz}|\propto\vec{i}_G\cdot\vec{E}_{THz}$.

While the phase matching conditions are the same for the chiral and quadrupolar processes, the angle dependence for the quadrupole process is such that the intensity vanishes when the grating wavevector is parallel to the incident optical radiation. Ignoring the phase matching requirements, the angular dependence [see Fig. 1(c)] of the radiated sideband power, $P_\pm$, will appear as follows:

$$\text{Quadrupolar process } P_\pm\propto[\cos(\theta_G-\theta_T)\sin(\theta_G)]^2,$$

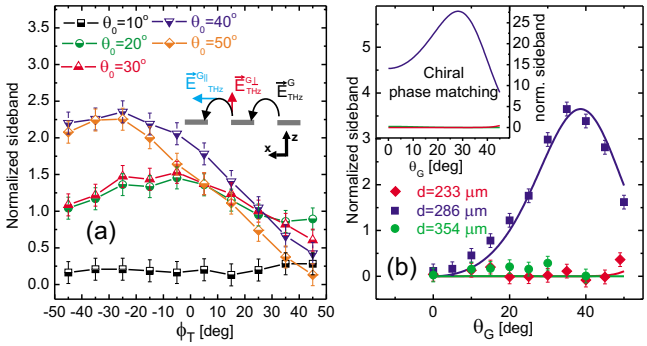

FIG. 3. (Color online) (a) Sideband intensity as a function of the polarization angle of the incident radiation for different rotations of the grating. Inset: the terahertz electric field lines near the grating connect the neighboring grating lines and terminate on the induced oscillating charges. The near grating terahertz field has both parallel and perpendicular components spatially modulated by the grating. (b) Measured and calculated sideband power at 0.675 THz vs grating angle for three different grating periods. Inset: calculated chiral dipolar sideband power; the same parameters.

$$\text{Chiral process } P_{\pm} \propto [\cos(\theta_G - \theta_T)\cos(\theta_G)]^2. \tag{4}$$

From this we, see that chiral dipolar and quadrupolar SDFG can be measured independently in this setup. Figure 3(a) shows a record of the angular dependence of the limonene sideband power as the polarization of the terahertz radiation is varied for various angular positions of the grating. As expected, for any orientation of the grating, the strongest mixing signal occurred for terahertz radiation perpendicular to the grating lines, along the grating wavevector. Treating phase matching, we obtain the following expression for the power of the SDFG radiation emitted from the quadrupolar polarization:

$$P_{\pm} \propto [\cos(\theta_G)\sin(\theta_G)]^2 \exp\left\{-\tfrac{1}{2}L_x^2[n_s k_0 + k_G \cos(\theta_G - \theta) - n_s k_{\pm}]^2\right\}. \tag{5}$$

Figure 3(b) shows the measured intensity versus grating orientation for several different grating periods. Phase matching requirements lead to a strong dependence on the grating period: only the 286 μm period grating produces appreciable scattering with 0.675 THz radiation. Despite being extremely sensitive to n_s and k_G, the experimental angle dependence is faithfully reproduced by the model assuming a very reasonable interaction length between the terahertz and optical beams of 1.5 mm along the optical beam. These facts taken with the total lack of signal without the liquid indicates that we are observing terahertz/optical, quadrupole/magnetic dipole allowed SDFG in the liquid.

It is important for future work to note [inset in Fig. 3(b)] that the chiral allowed SDFG yields a power dependence identical to Eq. (5) except for the $\sin(\theta_G)$ in the prefactor of the exponential, which is replaced by $\cos(\theta_G)$ [refer to Eq. (4)]. Thus, unlike the quadrupolar SDFG, the chiral dipolar SDFG process is not suppressed at zero grating angle and it is possible to distinguish chiral dipolar and quadrupolar allowed processes.

The observed signal is not unique to limonene but has also been observed in several other polar and nonpolar liquids. Table I compares the experimentally observed hyperpolarizabilities $\bar{\beta}=(1000N_A c_l/\epsilon_0)^{-1}\chi^{(2)}$ for limonene, carbon tetrachloride (CCl_4), and water, where N_A is the Avogadro's constant, ϵ_0 is the dielectric constant, and c_l is the molar concentration of the liquid. We keep the interaction volume the same but have not corrected for different terahertz absorption coefficients. This correction is most important for water and can be as large as factors of 2–3. The absolute values were determined from a comparison to the terahertz/optical sideband generation measured in a bismuth germanate crystal, placed directly onto the grating, in the same setup ($\chi^{(2)}=5\times10^{-12}$ m/V). For limonene and CCl_4, the measured signal reaches values similar to hyperpolarizabilities found for chiral dipole allowed SDFG of resonantly excited C–H bonds.[1]

TABLE I. Measured hyperpolarizabilities.

Liquid	M (mol/l)	$\lvert\bar{\beta}_{\text{quad}}\rvert$ (m^3 C/V^2)
Limonene	6.17	1.0×10^{-53}
CCl_4	10.27	0.5×10^{-53}
Water	55.35	0.05×10^{-53}

An estimate based on the work in Ref. 13 of the strength of chiral, electric dipole terahertz/visible SDFG gives hyperpolarizabilities about 20–1000 times larger than in Table I for single and double resonant excitation, respectively. This should place even protein solutions with molarities in the range of 10^{-3}–10^{-4} above our detection limit and thus provide a direct spectroscopy tool for macromolecular vibrations of biopolymers.

T.F. would like to thank the Alexander von Humboldt Foundation for the financial support. We gratefully acknowledge the help of Kevin Plaxco with all things touching (bio)chemistry. This work was supported by the (U.S.) Army Research Office under Contract No. W911NF0610241 and by the William M. Keck Foundation under Contract No. SB080017.

[1] M. A. Belkin, T. A. Kulakov, K.-H. Ernst, L. Yan, and Y. R. Shen, Phys. Rev. Lett. **85**, 4474 (2000).
[2] M. A. Belkin and Y. R. Shen, Int. Rev. Phys. Chem. **24**, 257 (2005).
[3] J. Xu, K. W. Plaxco, and S. J. Allen, J. Chem. Phys. **124**, 036101 (2006).
[4] J. Xu, K. W. Plaxco, and S. J. Allen, J. Phys. Chem. B **110**, 24255 (2006).
[5] U. Heugen, G. Schwaab, E. Bründermann, M. Heyden, X. Yu, D. M. Leitner, and M. Havenith, Proc. Natl. Acad. Sci. U.S.A. **103**, 12301 (2006).
[6] B. Born, S. J. Kim, S. Ebbinghaus, M. Gruebele, and M. Havenith, Faraday Discuss. **141**, 161 (2009).
[7] B. Born, H. Weingärtner, E. Brändermann, and M. Havenith, J. Am. Chem. Soc. **131**, 3752 (2009).
[8] J. A. Giordmaine, Phys. Rev. **138**, A1599 (1965).
[9] Y. R. Shen, *The Principles of Nonlinear Optics*, 1st ed. (Wiley, New York, 1984).
[10] P. Guyot-Sionnest and Y. R. Shen, Phys. Rev. B **38**, 7985 (1988).
[11] Quadrupolar and magnetic dipolar processes are very similar in nature and we do not attempt to distinguish them here.
[12] E. Adler, Phys. Rev. **134**, A728 (1964).
[13] P. Fischer, A. D. Buckingham, and A. C. Albrecht, Phys. Rev. A **64**, 053816 (2001).